M-type KCNQ2–KCNQ3 potassium channels are modulated by the KCNE2 subunit

Norbert Tinel, Sylvie Diochot, Inger Lauritzen, Jacques Barhanin, Michel Lazdunski, Marc Borsotto*

Institut de Pharmacologie Moléculaire et Cellulaire, CNRS-UPR 411, 660 route des Lucioles, Sophia Antipolis, 06560 Valbonne, France

Received 20 June 2000; revised 21 July 2000; accepted 28 July 2000

Edited by Pierre Jolles

Abstract KCNQ2 and KCNQ3 subunits belong to the six transmembrane domain K^+ channel family and loss of function mutations are associated with benign familial neonatal convulsions. KCNE2 (MirP1) is a single transmembrane domain subunit first described to be a modulator of the HERG potassium channel in the heart. Here, we show that KCNE2 is present in brain, in areas which also express KCNQ2 and KCNQ3 channels. We demonstrate that KCNE2 associates with KCNQ2 and/or KCNQ3 subunits. In transiently transfected COS cells, KCNE2 expression produces an acceleration of deactivation kinetics of KCNQ2 and of the KCNQ2–KCNQ3 complex. Effects of two previously identified arrhythmogenic mutations of KCNE2 have also been analyzed.

Key words: Potassium channel; Epilepsy; Regulatory protein; Immunoprecipitation; In situ hybridization

1. Introduction

The KCNQ family of potassium channels belonging to the six transmembrane domain group, was recently described. This family comprises five members, called KCNQ1 (KvLQT1) to KCNQ5.

KCNQ1 is highly expressed in heart [1]. It is associated with the regulatory protein KCNE1 (IsK) to produce the cardiac slow delayed rectifier (IKs) current [2,3]. KCNQ2 [4,5] and KCNQ3 [6] are expressed in the same brain areas such as hippocampus, neocortex and cerebellum [5,7,8]. KCNQ4 is strongly expressed in the inner ear [9,10]. KCNQ5 is found in brain and sympathetic ganglia [11,12]. Heteromultimeric associations of KCNQ2 with KCNQ3 and KCNQ4, and KCNQ3 with KCNQ5 are thought to correspond to the M-current, a muscarinic sensitive voltage- and time-dependent potassium current expressed in a variety of neuronal cell types [9,11–13].

Except for KCNQ5, all of the known KCNQ channels described to date are associated with inherited diseases. KCNQ1 is responsible for inherited cardiac long QT syndromes [1,14–16]. KCNQ2 and KCNQ3 are both linked to benign familial neonatal convulsions (BFNC) [4,6,7]. KCNQ4 is linked to a non-syndromic dominant deafness form, DFNA2 [9].

Recently, KCNE2 (MirP1) was described to be the partner of the HERG potassium channel in the heart where the combination could underlie the native cardiac I_{kr} current [17]. We analyzed the KCNE2 tissue distribution using a human cDNA panel, and we found that KCNE2 substantially expressed in human brain. The localization of KCNE2 RNAs using in situ hybridization analysis shows that it is expressed in the same brain regions that also express KCNQ2 and KCNQ3 [5]. This observation evidently led to the hypothesis that KCNE2 might modulate KCNQ2 and KCNQ3 channel activities. Immunoprecipitation experiments have indeed shown that KCNE2 is associated with both KCNQ2 and KCNQ3 subunits. Moreover KCNE2 has been shown to regulate the KCNQ2 and/or KCNQ3 channel activities by modulating their deactivation kinetics. The effects of the native KCNE2 subunit are changed when it is substituted by KCNE2 mutants which are described to be associated with long QT syndrome and ventricular fibrillation [17].

2. Materials and methods

2.1. Amplification

KCNE2 (GenBank clone, accession number AP000052) was amplified from human brain cDNAs using the polymerase chain reaction (PCR) performed with primers KCNE2-M AGCGAATTCGAAGCATGTCTACTTTATCC and KCNE2-T CTTTTGTCGACTATCAGGGGGACATTT. The amplification profile was 94°C, 1 min, 55°C, 1 min, 72°C, 1 min, 35 cycles. PCR products were subcloned into pCI-IRES-CD8 mammalian expression vector and checked by sequencing.

2.2. Tissue distribution

A panel of human tissue cDNAs (Clontech) was used as a template for PCR distribution analysis of the KCNE2 and KCNE1 (IsK). PCR primers used were KCNE2-M and KCNE2-T, IsK-A, TGCAGCAGTGGAACCTTAAT and IsK-B, TAGCCAGTGGTGGGGTTCA for KCNE2 and KCNE1. The PCR profile was: 94°C, 3 min, 94°C, 40 s, 55°C, 1 min, 72°C, 1 min 30 s, 28 cycles.

PCR products were electrophoresed and blotted onto Hybond-N^+ membranes (Amersham), and probed with KCNE2 full length or with IsK-C, GTCGTGCTATGTCGTTGAAAATCT.

2.3. In situ hybridization

Antisense and sense RNA probes were generated from linearized plasmids containing the full length KCNE2 cDNA. Tissue preparation and hybridization were performed as described in [18]. The hybridization temperature was 50°C. Specimens were exposed to Amersham β-max Hyperfilm for 7 days.

Selected slides were subsequently dipped in photographic emulsion (LM-1, Amersham), incubated for 4 weeks, and then developed in Kodak D-19. Rat brain structures were identified according to Paxinos and Watson [19].

2.4. Coimmunoprecipitation

c-myc-Tagged KCNE2 was prepared by PCR using KCNE2-M and

*Corresponding author. Fax: (33)-4-93 95 77 04.
E-mail: borsotto@ipmc.cnrs.fr

Abbreviations: PCR, polymerase chain reaction; BFNC, benign familial neonatal convulsions

0014-5793/00/$20.00
PII: S0014-5793(00)01918-9

KCNE2-c-myc oligonucleotides GATATCACAGATCCTCTTCTG-AGATGAGTTTTTGTTCGGGGGACATTTTGAACCCAGC.

Proteins were in vitro translated (TNT system, Promega) with ^{35}S-methionine (ICN) as a radioactive marker, starting with 2 μg of each plasmid (pCI-KCNE2-c-myc, pCI-KCNQ2, pCI-KCNQ3 and pCI-Kv4.2) per 50 μl final reaction. Proteins were then five fold diluted with a buffer containing 150 mM NaCl, 50 mM Tris–HCl pH 7.4, 1 mM iodoacetamide, 1× mixture of protease inhibitors (Roche) and 1.5% Tween 20.

An equal volume of each in vitro translation was mixed and incubated 4 h on ice and then immunoprecipitated with an anti-c-myc monoclonal antibody (9E10 Santa Cruz Biotechnology) immobilized on protein-A–Sepharose gel (Amersham Pharmacia). Immunoprecipitates were analyzed on 12% SDS–PAGE.

2.5. Electrophysiological measurements in transfected COS cells

COS-7 cells were grown and transfected as described in [5] with 1 μg or 0.5 μg (in the coexpression experiments) of pCI-IRES-CD8-KCNE2 and pCI-KCNQ2 or pCI-KCNQ3 per dish. Cells were tested in electrophysiological experiments 48 h post transfection.

Electrophysiological recordings were carried out at 22 ± 2°C in the whole-cell configuration of the patch-clamp technique. The intracellular pipette filling solution contained 150 mM KCl, 0.5 mM $MgCl_2$, 5 mM EGTA and 10 mM HEPES–KOH at pH 7.4 and the standard extracellular solution contained 150 mM NaCl, 5 mM KCl, 1 mM $CaCl_2$, 3 mM $MgCl_2$, 5 mM glucose and 10 mM HEPES–NaOH at pH 7.4.

Data analysis allowed the presentation of values as the mean ± S.E.M. for the density (pA/pF), the voltage dependence of activation ($V_{0.5}$ in mV, and slope factor), and activation and deactivation kinetics (τ_{act} and τ_{deac} in ms) of the currents.

3. Results

3.1. KCNE2–KCNE1 sequence comparison

KCNE2 presents 51.2% of overall conservative homology with KCNE1 with a highly conserved region, amino acids 50–100, which shares 72% homology (Fig. 1A). The two potential *N*-glycosylation sites identified in the KCNE1 sequence are also present in the KCNE2 sequence but a deletion of 11 amino acids at position 102 results in a loss of one of the two phosphorylation sites for protein kinase C identified in the KCNE1 sequence (Fig. 1A).

3.2. Tissue distribution of human KCNE2

The tissue distribution of human KCNE2 mRNAs indicates that KCNE2 is more widely distributed than KCNE1 (Fig. 1B). KCNE2 expression is highest in brain, heart, skeletal muscle, pancreas, placenta, kidney, colon and thymus. A small but significant expression is found in liver, ovary, testis, prostate, small intestine and leukocytes. KCNE2 expression is very low, nearly undetectable, in lung and spleen.

3.3. Localization of KCNE2 in the rat brain by in situ hybridization

Hybridization with a KCNE2 probe reveals a very intense signal in the 4th and lateral ventricles (Fig. 2A–C). This intense labelling is not related to a neuronal expression (Fig. 2F). In addition, a neuronal expression is observed in cerebellum (Fig. 2A), neocortex, piriform cortex (Fig. 2B), the hippocampal formation, thalamus, hypothalamus, zona incerta, and various unidentified brainstem nuclei (Fig. 2C).

In cerebellum, both granule and Purkinje neurons are labelled (Fig. 2D). A moderate to strong signal is seen in all layers of the neocortex (Fig. 2E). Within the hippocampus, transcripts are abundant in both pyramidal neurons throughout the Ammon's horn and in dentate gyrus granule neurons (Fig. 2G).

No signal was seen when sections were hybridized with the corresponding sense riboprobe (data not shown).

3.4. Immunoprecipitation

First, we checked that KCNE2-c-myc displayed the same

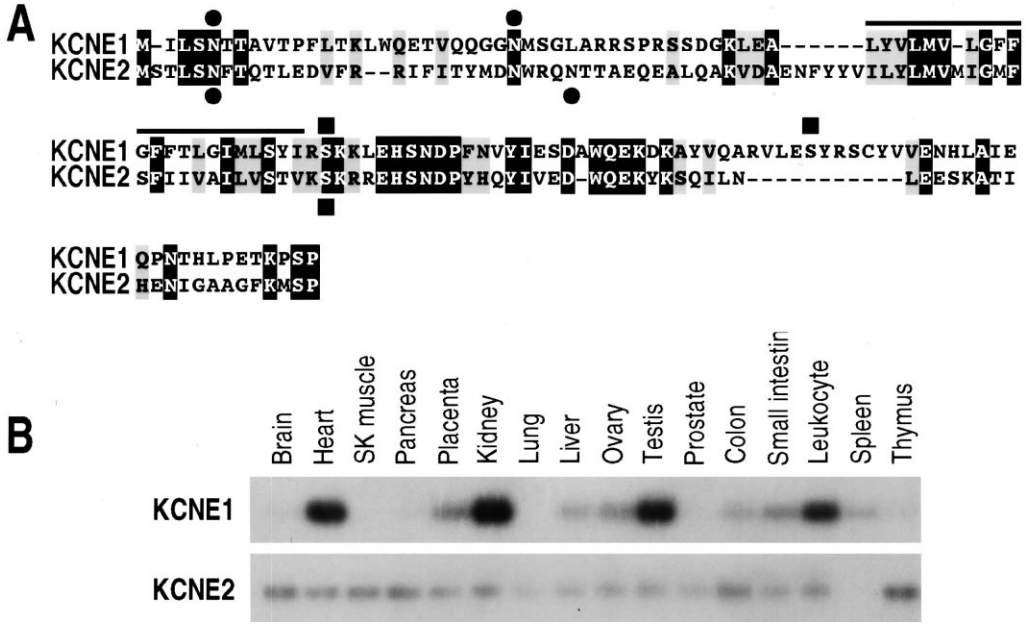

Fig. 1. Sequence and tissue distribution comparisons between KCNE1 and KCNE2. A: Sequence comparison between KCNE1 and KCNE2 proteins. Alignment of human KCNE1 and human KCNE2 protein sequences. Identical and conservative residues are boxed black and gray, respectively. Gaps are introduced to display the best alignment. The transmembrane domain is underlined by a bar. Filled circles indicate *N*-glycosylation sites and filled squares, phosphorylation sites of protein kinase C. B: Tissue distribution comparison between KCNE1 RNA and KCNE2 RNA.

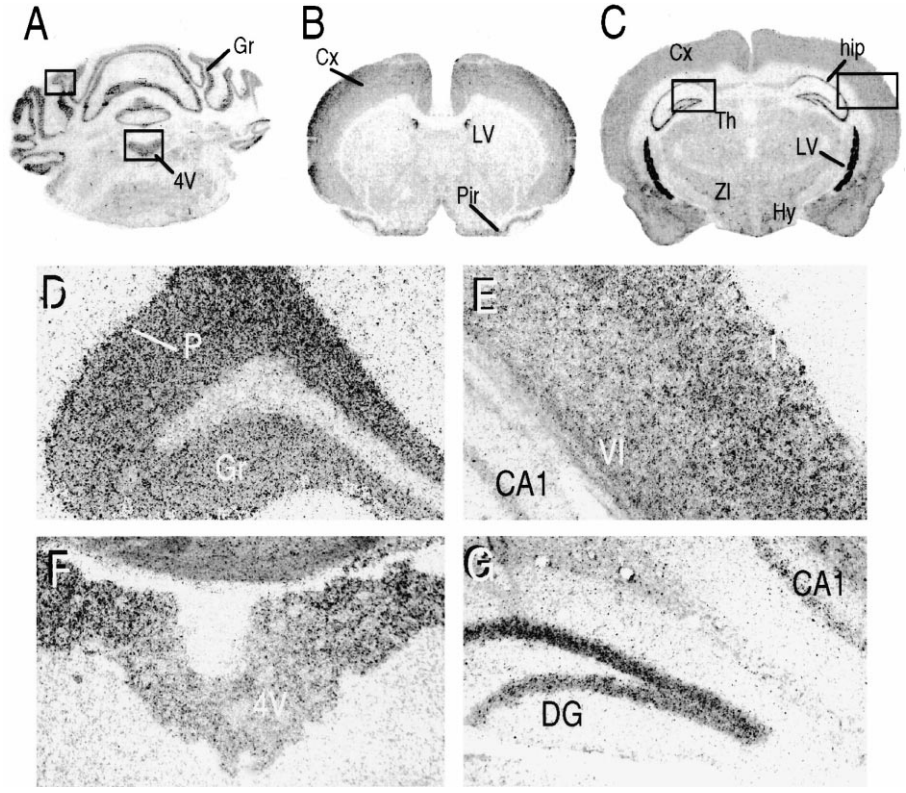

Fig. 2. In situ hybridization of KCNE2. Localization of KCNE2 mRNA in the adult rat brain. A–C: Autoradiograms of rat coronal brain sections after in situ hybridization with the KCNE2 riboprobe. D–G: high power images of photomicrographic emulsion dipped slices at level of the (D) cerebellar granule layer, E: neocortex, F: 4th ventricle and G: hippocampus. CA1: pyramidal cell layer, Cx: neocortex, DG: dentate gyrus, Gr: cerebellar granule cell layer, hip: hippocampus, Hy: hypothalamus, LV: lateral ventricle, Pir: piriform cortex, Th: thalamus.

ability as the native KCNE2 to modulate KCNQ channel activities (data not shown).

When in vitro translated KCNE2-c-myc is mixed either with in vitro translated KCNQ2 or KCNQ3, the c-myc monoclonal antibody immunoprecipitates both KCNE2 and KCNQ channel subunits (Fig. 4, lanes 2 and 3). No KCNQ2 immunoprecipitation was obtained in the absence of KCNE2 in the mixture (Fig. 3, lane 5). Under the same experimental conditions, the Kv4.2 channel does not coprecipitate with KCNE2-c-myc (Fig. 3, lane 4).

3.5. *Effects of the KCNE2 subunit on the electrophysiological properties of KCNQ2 or KCNQ3 currents*

The whole-cell voltage clamp technique was used for current recordings in transiently transfected COS cells. In our expression conditions both KCNQ2 and KCNQ3 are able to produce active K^+ currents. The combination KCNQ2+KCNQ3 results in the expression of a new current that can be discriminated from each independent current by its voltage dependence of activation and by its time constant of activation (Table 1).

Table 1
Electrophysiological parameters of KCNQ2, KCNQ3 currents and heteromultimers associated or not with the KCNE2 protein or its mutants

Channel type	Current Density (pA/pF)	Activation curve		Time constant of activation (ms)	Time constant of deactivation (ms)
		$V_{0.5}$ (mV)	Slope (mV)		
KCNQ2	12.1 ± 1.4 (16)	−26.1 ± 1.3 (14)	13.2 ± 0.8 (14)	156.7 ± 9 (14)	236 ± 9.9 (12)
KCNQ2+KCNE2	15.2 ± 2.8 (7)	−29 ± 1.8 (12)	13.3 ± 1.1 (12)	110.8 ± 11.3 (10)***(a)	156 ± 6.1 (12)***(a)
KCNQ2+KCNE2-Q9E	10.8 ± 1.7 (10)	−30.7 ± 1.6 (11)	11.6 ± 0.8 (11)	90 ± 4.2 (10)	190 ± 5.5 (10)***(b)
KCNQ2+KCNE2-I57T	16.8 ± 5.9 (7)	−25.6 ± 3.8 (7)	13.6 ± 1.6 (7)	117 ± 12 (7)	227 ± 17.3 (7)***(b)
KCNQ3	11.2 ± 2.8 (13)	−39 ± 1.4 (9)	7.9 ± 1.3 (9)	60.6 ± 4.9 (9)	178 ± 25 (6)
KCNQ3+KCNE2	7.8 ± 3 (6)	−32.7 ± 3.2 (6)	5.9 ± 2 (6)	47.3 ± 12 (6)	255 ± 70 (5)
KCNQ2+KCNQ3	13.6 ± 1.2 (18)	−30.6 ± 0.9 (21)	13.9 ± 0.7 (21)	134.3 ± 5.7 (23)	180.2 ± 8.3 (20)
KCNQ2+KCNQ3+KCNE2	18 ± 2.6 (13)	−25.6 ± 1.4 (17)***(c)	13.4 ± 0.6 (17)	99.5 ± 4.6 (17)***(c)	103 ± 5.4 (15)***(c)
KCNQ2+KCNQ3+KCNE2-Q9E	16.2 ± 2.1 (10)	−23 ± 1.7 (11)	12.1 ± 0.7 (11)	108.4 ± 9.4 (10)	117.4 ± 8.7 (7)
KCNQ2+KCNQ3+KCNE2-I57T	21.6 ± 3.3 (11)	−25.6 ± 1.7 (10)	18.6 ± 1.8 (10)***(d)	68 ± 6 (9)***(d)	118 ± 6 (9)

Values between brackets indicate the number of cells tested.
Statistically significant differences were assessed by mean of a Student's *t*-test, with values obtained from (a) KCNQ2, (b) KCNQ2+KCNE2, (c) KCNQ2+KCNQ3 and (d) KCNQ2+KCNQ3+KCNE2 (***, $P < 0.005$).

The interaction of the KCNE2 subunit with the KCNQ2 channel subunit results in an acceleration of the deactivation kinetics of the current. Time constants of deactivation at −40 mV are decreased from $\tau_{deac} = 236 \pm 9.9$ ms ($n = 12$) to 156 ± 6.1 ms ($n = 12$) for KCNQ2 and KCNQ2+KCNE2 respectively (Fig. 4A,C). The activation kinetics are also accelerated although in a lesser extent, by the presence of the KCNE2 subunit. At +30 mV, $\tau_{act} = 156.7 \pm 9$ ms ($n = 14$) and 110.8 ± 11.3 ms ($n = 10$) for KCNQ2 and KCNQ2+KCNE2 channels, respectively.

The KCNE2 subunit does not alter significantly the voltage dependence of activation of the KCNQ2 current recorded in COS cells (Table 1).

The electrophysiological properties of the KCNQ3 channel were not significantly altered by the interaction with the KCNE2 subunit (Table 1).

3.6. *KCNE2 associates with heteromultimers KCNQ2+KCNQ3*

Representative traces recorded in cells expressing KCNQ2+KCNQ3 in the absence or the presence of KCNE2 are shown in Fig. 4B.

As observed with KCNQ2 alone, coexpression of KCNE2 with KCNQ2+KCNQ3 results in an acceleration of both the activation and deactivation processes. The time constant of activation at +30 mV is $\tau_{act} = 99.5 \pm 4.6$ ms in the presence of KCNE2 versus 134.3 ± 5.7 ms in its absence ($n = 40$, $P < 0.005$), and the time constant of deactivation at −40 mV changes from 180.2 ± 8.3 ms to 103 ± 5.4 ms ($n = 35$, $P < 0.005$) (Fig. 4D and Table 1). While KCNE2 coexpression shifted the voltage dependence of activation to more negative values, it shifted the $V_{0.5}$ of KCNQ2+KCNQ3 activation by about 5 mV towards positive values (Table 1). Coexpression of the KCNE2 subunit did not affect significantly the mean current density (Fig. 4E,F and Table 1).

3.7. *Effects of KCNE2 arrhythmogenic mutations*

KCNE2 mutations have been reported to be linked to cardiac arrhythmia [17]. We have introduced two of them, I57T and Q9E, in the KCNE2 sequence to analyze their effects on KCNQ2 and KCNQ2+KCNQ3 currents. It appears that each mutation has specific effects on the biophysical properties of these currents (see Table 1). As a general rule these mutations tend to reduce the kinetic effects of the wild type KCNE2, excepted for KCNE2-I57T which accelerates the current activation of KCNQ2+KCNQ3 channels (Table 1).

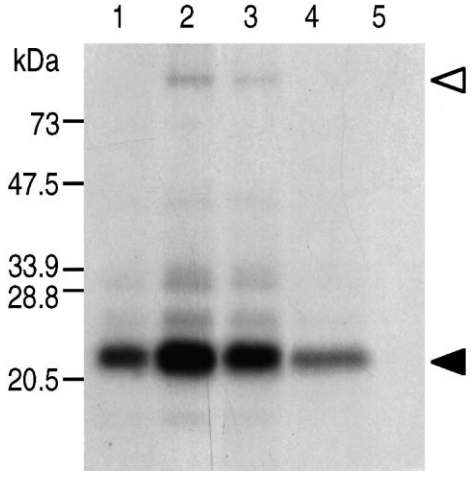

Fig. 3. KCNE2 immunoprecipitation. 12% SDS–PAGE analysis of in vitro translations immunoprecipitated with a c-myc monoclonal antibody. KCNE2-c-myc alone (lane 1), KCNE2-c-myc+KCNQ2 (lane 2), KCNE2-c-myc+KCNQ3 (lane 3), KCNE2-c-myc+Kv4.2 (lane 4), KCNQ2 alone (lane 5).

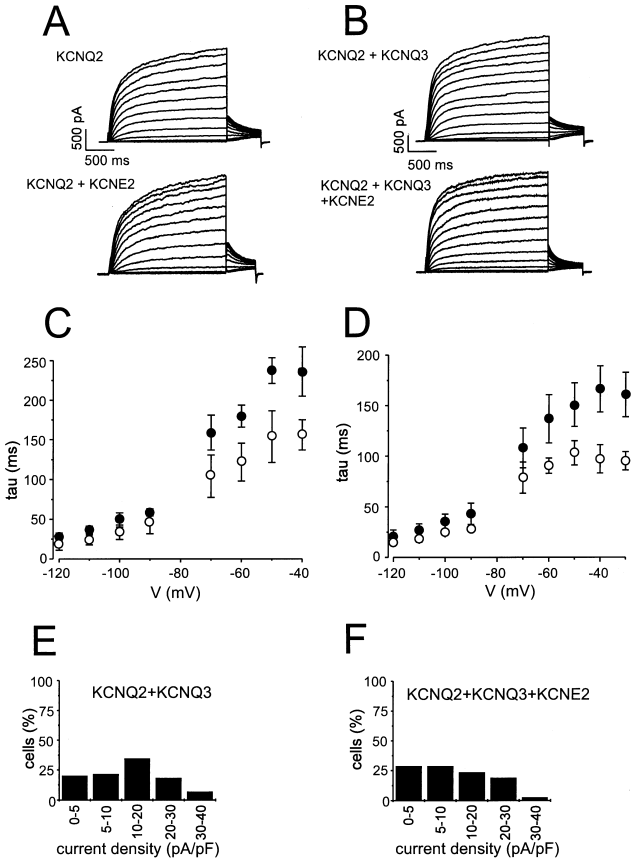

Fig. 4. KCNE2 subunit associates with KCNQ2 and KCNQ2+KCNQ3 channels in COS cells. Currents were recorded in transfected COS cells in the whole-cell configuration. Current densities were calculated for each channel combination, only cells expressing currents larger than 5 pA/pF were considered in this calculation. A and B: Representative traces for (A) KCNQ2 and KCNQ2+KCNE2 currents, and (B) KCNQ2+KCNQ3, and KCNQ2+KCNQ3+KCNE2 currents. Traces were elicited by 2 s voltage steps from a holding potential of −80 mV over the range of −60–+60 mV in 10 mV increment. C and D: Time constants of deactivation (τ_{deac} in ms) are calculated from tail currents elicited from −120 to −40 mV in 10 mV increment after a test pulse to +30 mV. C: KCNQ2 (filled circle), KCNQ2+KCNE2 (open circle). D: KCNQ2+KCNQ3 (filled circle) and KCNQ2+KCNQ3+KCNE2 (open circle). E and F: Histograms of the percentage of cells producing indicated current densities for (E) KCNQ2+KCNQ3 and (F) KCNQ2+KCNQ3+KCNE2. The current density (pA/pF) was calculated for each recorded cell in relation with the capacitance and the peak current amplitude at +30 mV. Averaged current densities were compared in each combination with Student's *t*-test. Mean values are not significantly modified with the KCNE2 expression with current densities of 11.82 ± 1.04 for KCNQ2+KCNQ3 ($n = 44$), and of 11.76 ± 1.55 for KCNQ2+KCNQ3+KCNE2 ($n = 35$), $P = 0.97$.

4. Discussion

KCNE2 shows a strong overall conservative homology with KCNE1. A notable difference between these two proteins, is a deletion of 11 amino acids at position 102 of KCNE2 which

leads to a loss of a phosphorylation site for protein kinase C, described to be important for the regulation of KCNE1 activity [20,21]. Nevertheless, the sequence comparison clearly indicates that KCNE2 is a member of the KCNE family and thus could potentially interact with a KCNQ potassium channel like KCNE1 does [2,3,22]. However, KCNE1 and KCNE2 present important differences in their tissue distribution. The expression of KCNE2 in the brain led us to analyze the localization of KCNE2 in the central nervous system. The overall distribution of the KCNE2 mRNA in the rat and mouse central nervous systems was similar to that described earlier for KCNQ2 and KCNQ3 in mouse brain [5]. Heteromultimers of these two K^+ channel subunits are thought to have an important role in the central nervous system where they are believed to form the M-type K^+ channel [9,13] and are both linked to a familial form of newborn epilepsy [4,6,7]. The apparent colocalization of KCNQ2, KCNQ3 and KCNE2 suggested that KCNE2 could be a good candidate as a regulatory subunit of the KCNQ2–KCNQ3 M-type channel. We present arguments in favor of such a hypothesis. First, KCNQ2 and KCNQ3 subunits can be specifically coimmunoprecipitated with KCNE2 under in vitro conditions. Second, electrophysiological studies performed in COS cells, show that the deactivation kinetics of either KCNQ2 or KCNQ2 associated with KCNQ3 channels are increased by the coexpression of the KCNE2 subunit. Although these effects are not as spectacular as those of KCNE1 on KCNQ1, they are highly significant ($P < 0.005$). Moreover, they are very similar to those reported for KCNE2 modulating effects on the HERG channel [17].

Missense mutations have been found in the KCNE2 gene from patients with long QT syndrome, that modulate KCNE2 effects on the HERG channel [17]. We found that KCNE2-I57T and KCNE2-Q9E mutants partially or totally reversed the effect of the native KCNE2. This partial or total loss of KCNE2 function induced by these mutations could indicate that patients with such mutations can, in addition to the long QT disease, also present neurological disorders.

All our data including in situ localization and in vitro physical and functional interactions argue in favor of an association between the KCNQ2 and KCNQ3 channels and KCNE2 subunit. Data from literature also support this finding. The native M-current thought to be formed by the association of KCNQ2 with KCNQ3, displays deactivation kinetics faster than those recorded in the heterologous expression experiments [13]. It was reported that the heterologously expressed KCNQ2+KCNQ3 current had a deactivation time constant of $\tau_{deac} = 174$ ms, a value very similar to the one found in the present study (180 ms, Table 1). In the same study [13], the deactivation time constant of native M-current was evaluated to $\tau_{1deac} = 103$ ms (at -50 mV), a value almost identical to the τ_{1dea} conferred by the association of the KCNE2 subunit to the KCNQ2+KCNQ3 complex (Table 1). Hence, channels formed by the association of the three subunits appropriately recapitulate native M-current.

Acknowledgements: This work was supported by the Centre National de la Recherche Scientifique (CNRS), the Conseil Regional (PACA) and by the Association Francaise contre les Myopathies (AFM). We thank Dr A. Patel for reading the manuscript, M. Jodar, N. Leroudier, F. Aguila for expert technical assistance and V. Lopez for secretarial assistance.

References

[1] Wang, Q. et al. (1996) Nature Genet. 12, 17–23.
[2] Barhanin, J., Lesage, F., Guillemare, E., Fink, M., Lazdunski, M. and Romey, G. (1996) Nature 384, 78–80.
[3] Sanguinetti, M.C., Curran, M.E., Zou, A., Shen, J., Spector, P.S., Atkinson, D.L. and Keating, M.T. (1996) Nature 384, 80–83.
[4] Singh, N.A. et al. (1998) Nature Genet. 18, 25–29.
[5] Tinel, N., Lauritzen, I., Chouabe, C., Lazdunski, M. and Borsotto, M. (1998) FEBS Lett. 438, 171–176.
[6] Charlier, C., Singh, N.A., Ryan, S.G., Lewis, T.B., Reus, B.E., Leach, R.J. and Leppert, M. (1998) Nature Genet. 18, 53–55.
[7] Biervert, C., Schroeder, B.C., Kubisch, C., Berkovic, S.F., Propping, P., Jentsch, T.J. and Steinlein, O.K. (1998) Science 279, 403–406.
[8] Yang, W.P., Levesque, P.C., Little, W.A., Conder, M.L., Ramakrishnan, P., Neubauer, M.G. and Blanar, M.A. (1998) J. Biol. Chem. 273, 19419–19423.
[9] Kubisch, C., Schroeder, B.C., Friedrich, T., Lutjohann, B., El-Amraoui, A., Marlin, S., Petit, C. and Jentsch, T.J. (1999) Cell 96, 437–446.
[10] Trussell, L. (2000) Proc. Natl. Acad. Sci. USA 97, 3786–3788.
[11] Lerche, C., Scherer, C.R., Seebohm, G., Derst, C., Wei, A.D., Busch, A.E. and Steinmeyer, K. (2000) J. Biol. Chem. 27, 27.
[12] Schroeder, B.C., Hechenberger, M., Weinreich, F., Kubisch, C. and Jentsch, T.J. (2000) J. Biol. Chem. 17, 17.
[13] Wang, H.S., Pan, Z., Shi, W., Brown, B.S., Wymore, R.S., Cohen, I.S., Dixon, J.E. and McKinnon, D. (1998) Science 282, 1890–1893.
[14] Neyroud, N. et al. (1997) Nature Genet. 15, 186–189.
[15] Chouabe, C., Neyroud, N., Guicheney, P., Lazdunski, M., Romey, G. and Barhanin, J. (1997) EMBO J. 16, 5472–5479.
[16] Barhanin, J., Attali, B. and Lazdunski, M. (1998) Trends Cardiovasc. Med. 8, 207–214.
[17] Abbott, G.W., Sesti, F., Splawski, I., Buck, M.E., Lehmann, M.H., Timothy, K.W., Keating, M.T. and Goldstein, S.A. (1999) Cell 97, 175–187.
[18] Lesage, F., Lauritzen, I., Duprat, F., Reyes, R., Fink, M., Heurteaux, C. and Lazdunski, M. (1997) FEBS Lett. 402, 28–32.
[19] Paxinos, G. and Watson, C. (1986) The Rat Brain in Stereotaxic Coordinates, Academic Press, San Diego, CA.
[20] Busch, A.E., Varnum, M.D., North, R.A. and Adelman, J.P. (1992) Science 255, 1705–1707.
[21] Varnum, M.D., Busch, A.E., Bond, C.T., Maylie, J. and Adelman, J.P. (1993) Proc. Natl. Acad. Sci. USA 90, 11528–11532.
[22] Attali, B. (1996) Nature 384, 24–25.